Systematic investigation of sustained laser-induced incandescence in carbon nanotubes

Cite as: J. Appl. Phys. **107**, 064319 (2010); https://doi.org/10.1063/1.3359681
Submitted: 06 January 2010 . Accepted: 09 February 2010 . Published Online: 30 March 2010

Zhi Han Lim, Andrielle Lee, Kassandra Yu Yan Lim, Yanwu Zhu, and Chorng-Haur Sow

Systematic investigation of sustained laser-induced incandescence in carbon nanotubes

Zhi Han Lim,[1,2] Andrielle Lee,[1] Kassandra Yu Yan Lim,[3] Yanwu Zhu,[1] and Chorng-Haur Sow[1,2,a)]
[1]*Department of Physics, Faculty of Science, National University of Singapore, Singapore 117542, Singapore*
[2]*National University of Singapore Nanoscience and Nanotechnology Initiative, National University of Singapore, Singapore 117542, Singapore*
[3]*Hwa Chong Institution, 661 Bukit Timah Rd., Singapore 269734, Singapore*

(Received 6 January 2010; accepted 9 February 2010; published online 30 March 2010)

A focused laser beam irradiating on aligned carbon nanotubes (CNTs) in moderate vacuum results in bright and sustained laser-induced incandescence (LII) in CNTs. The incandescence corresponds to blackbody radiation from laser-heated CNTs at ~2400 K. Post-LII craters with well-defined ring boundaries in the CNT array were observed and examined with scanning electron microscopy and Raman spectroscopy. The enhanced purity of CNTs after LII as indicated by Raman spectroscopy studies was attributed to the removal of amorphous carbons on the as-grown CNTs during LII. A dynamic study of the crater formation further elucidates the nature of such craters. Through a systematic study of the effect of vacuum level and gaseous environment on LII, we discovered the process of thermal runaway during LII in CNTs. Thermal runaway is a threat to a sustained LII and can be prevented in nitrogen and argon environments. Oxygen was found to be responsible for thermal runaway reactions. © *2010 American Institute of Physics*. [doi:10.1063/1.3359681]

I. INTRODUCTION

The study of laser carbon nanotubes (CNTs) interactions is a growing field. The use of laser to impinge on CNTs had been found to result in various phenomena such as exfoliation,[1] purification,[2] morphological modifications,[3] trimming,[4] actuation,[5] and photoconductivity.[6] We have previously reported a postgrowth technique to create two-dimensional patterns and three-dimensional microstructures in vertically aligned multiwalled CNTs arrays.[7] This was achieved by the use of a strongly focused continuous wave laser beam to burn or destroy the local area of aligned CNTs below the focused laser spot. This technique is akin to laser pruning of CNTs, drawing the analogy of the pruning of plants in a garden landscape.

In the process of laser pruning, we typically see a bright flash of light emitted from the CNTs at the instant when the focused laser beam strikes the sample surface. We attribute this phenomenon to the CNTs dissipating heat via radiation. In order to study these flashes, we subjected the sample in vacuum as an attempt to reduce heat loss due to interactions with molecules in the air, thus enhancing the radiation. The results were pleasantly surprising—the flash became an intense glow, which could sustain for more than 2 h. The optical spectrum of the emissions was verified to be that of a blackbody radiation. In an earlier report, we called this phenomenon a sustained laser-induced incandescence (LII) in CNTs.[8]

The terminology "laser-induced incandescence" was derived from the well-known technique of heating primary particles with laser resulting in blackbody radiation emissions. LII of carbon soot was first reported in 1977 by Eckbreth[9] while performing Raman scattering diagnostics in flames. His initial studies were motivated by the noisy interferences caused by LII, which tend to overwhelm the desired Raman signals. Later in 1984, Melton[10] showed that LII could provide an efficient method to acquire the soot particle temperature, primary particle size distributions parameters and relative soot volume fraction. Today, LII is an emerging and practical technology for particle concentration and particle size measurements in combustion, particle synthesis, and environment applications.[11–13]

While experimental and theoretical works on LII of primary soot particles are abundant in the literature, little has been explored on extended carbon structures such as CNTs. There has been however isolated incidents of optically induced ignition of CNTs reported.[14–19] Our earlier report presents the details in the creation of sustained LII with a focused laser beam on aligned CNTs in a vacuum environment.[8] In this work, we extend our effort in the investigation of this phenomenon, by studying at the LII with CNTs in different controlled gaseous environments and examining the formation of post-LII craters left on the aligned CNTs arrays.

II. EXPERIMENTAL

CNTs used in this work are multiwalled and grown vertically aligned on a silicon substrate. Details of the growth process are described elsewhere.[20] Figure 1 shows a schematic of the experimental setup of optical microscope-focused laser beam system utilized in this work where sustained LII of CNTs can be achieved. The parallel laser beam from a diode laser (wavelength 663 nm, beam width 3 mm and maximum output power of 80 mW) was directed with mirrors into the optical microscope where the beam was fur-

a)Electronic mail: physowch@nus.edu.sg.

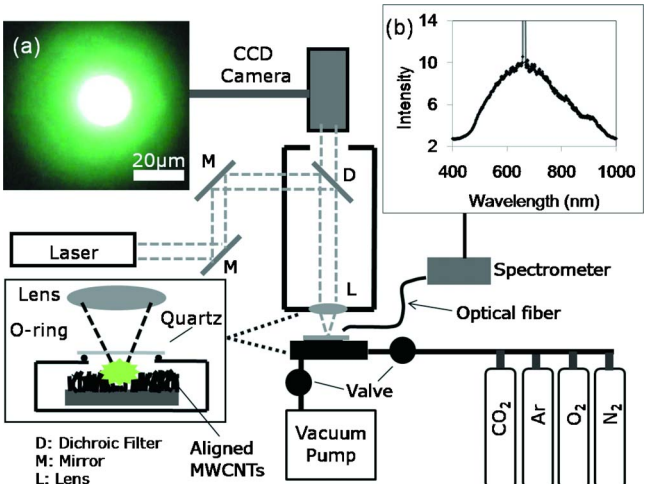

FIG. 1. (Color online) Setup of focused laser system where LII in CNTs is achieved. Insets (a) and (b) show the optical image and (as-captured) intensity profile of a typical LII of CNT, respectively.

ther deflected with a dichroic filter to reach the objective lens. Other lasers emitting laser beam with different wavelengths, namely 532, 632, and 1064 nm were also capable of inducing similar incandescence in CNTs. The 50× objective lens with a working distance of 8.3 mm focused the laser to a Gaussian beam, with a narrow beam waist of ~5 μm. With the long working distance, the space between the lens and the sample could fit a transparent vacuum chamber for the sample to sit in. The power of the laser beam after passing through the system of optics was reduced to ~30% of the original emitted power. The same objective lens was used to collect reflected and emitted light from the sample for viewing purposes. The optical image was captured by a charge-coupled device camera attached to the optical microscope system such that real time images under the microscope could be shown on the TV monitor and recorded (see videos of LII recorded in Ref. 21). To study the optical characteristics of the LII signals, an optical fiber that is part of an Ocean Optics optical spectrometer (USB4000) system was brought close to the sample, as shown in Fig. 1. The spectrometer recorded the LII intensities with a broadband of wavelengths ranging from 345 to 1000 nm. Calibration of the raw data was required due to the wavelength dependent detection efficiency of the spectrometer. A known light source (Ocean Optics LS-1-CAL) was used for this purpose. Insets (a) and (b) in Fig. 1 show the optical image and intensity profile of a typical LII of CNTs, respectively. Various gas cylinders could be connected to the vacuum chamber to subject the sample to different gaseous environments.

Sustained LII of CNTs was achieved upon the irradiation of the focused laser beam with a minimum incident power of 5 mW and a vacuum level of 1 mTorr or lower pressure. The emissions were broadband and bright enough to be seen by the unaided eyes. The origin of the intense light is attributed to incandescent effect where the sample dissipates the light energy it absorbs from the laser beam by radiation. Analysis of the optical spectrum shows a close fit to the Planck blackbody radiation equation as we shall detail in the next section.

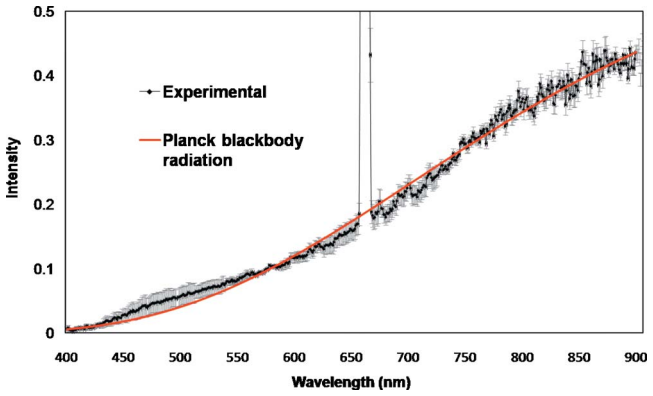

FIG. 2. (Color online) A typical (corrected) intensity profile of LII in CNTs. A rescaled Planck blackbody wavelength distribution function at $T=2450$ K provides an excellent fitting to the experimental data with a calculated reduced χ^2 value of 1.24.

III. RESULS AND DISCUSSIONS

A. Blackbody radiation

LII is a process whereby particles are heated by laser to an extent where it radiates blackbody emissions in visible light regime. Here we first show that the nature of LII in CNTs is indeed that of a blackbody radiation. The typical intensity profile of LII in CNTs, after corrected of the wavelength dependent detection efficiency of the spectrometer is shown in Fig. 2. The graph was fitted with a rescaled blackbody wavelength distribution function

$$I(\lambda) = A\frac{2\pi hc^2}{\lambda^5(e^{hc/\lambda k_B T}-1)}, \tag{1}$$

where I is the intensity of the LII at wavelength λ and T and A are the temperature and scaling factor obtained from the fitting, respectively. The scaling factor accounts for the geometry of the detection setup and the detection efficiency of the spectrometer. The best fit curve obtained with $T=2450$ K falls within the error bars of the experiment and has a calculated reduced χ^2 value of 1.24. The relatively good fit indicates that the observed emissions are indeed that of a hot blackbody radiation.

By operating the spectrometer in a continual time acquisition mode, we collected in real-time the variation of the intensity profile. Figure 3(a) shows a typical time evolution of LII intensity at selected wavelengths. By rearranging Eq. (1) and employing the approximation of $e^{hc/\lambda k_B T}-1$

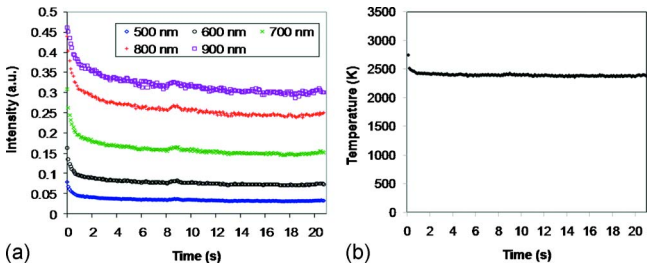

FIG. 3. (Color online) (a) Time evolution of LII intensity at selected wavelengths. (b) Evolution of temperature of the LII as calculated with Eq. (2) corresponding to the intensity data in (a). The focused laser beam irradiates on the sample from $t=0$ s.

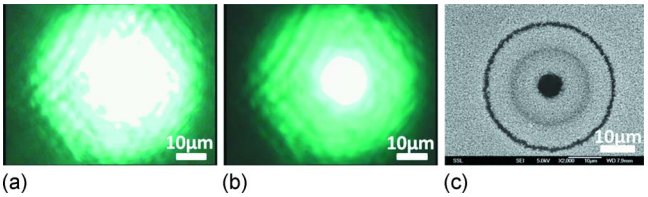

FIG. 4. (Color online) (a) Very bright LII just after the onset of laser. (b) Sustain glow of LII after ~20 s of continuous laser irradiation. (c) SEM image of a crater formed during LII.

$\approx e^{hc/\lambda k_B T}$, one can express temperature as the subject, as shown in Eq. (2), such that the temperature of the incandescence at each time step can be conveniently obtained,

$$T = \frac{hc}{k_B} \frac{1/\lambda_1 - 1/\lambda_2}{\ln(\lambda_2^5 I_2) - \ln(\lambda_1^5 I_1)}. \quad (2)$$

Figure 3(b) shows the evolution of the temperature of the LII corresponding to the intensity data in Fig. 3(a) using $(\lambda_1, \lambda_2) = (500\ \text{nm}, 800\ \text{nm})$. The continuous laser beam starts to irradiate on the sample at $t = 0$ s. It is noted that any other pairs of wavelengths (except those in the vicinity of the laser wavelength 663 nm) are just as adequate in obtaining the temperature evolution. We emphasize here that the temperature of the incandescence achieved was very high, reaching >2700 K immediately after laser irradiation and maintaining a sustained temperature of ~2380 K subsequently. This is compared with recently reported incandescent light emission from CNTs by joule heating,[22,23] where the temperature of incandescence ranged from 900 to 1600 K, dependent on the magnitude of the source current. In our work, the heat source is generated by a focused laser beam instead. This enables precise control over the position of the localized incandescence and suggests that LII of CNTs can serve as a technique to perform instantaneous localized high temperature heating in a microsized region of the CNT array.

B. Post-LII craters

A striking feature of LII in aligned CNTs is the formation of a crater with concentric-rings pattern in the CNT array. Figure 4 shows the following sequence of events: (a) the very bright LII just after the onset of laser, (b) the sustained glow of LII after ~20 s of continuous laser irradiation, and (c) the crater formed after the laser beam was removed. The appearance of the post-LII crater was not anticipated despite our prior experience in laser pruning of aligned CNT arrays. The action of the focused laser beam on aligned CNT in room ambient conditions results in a conical hole burnt into the CNT array. This was the basis of the laser pruning technique and we expected a similar outcome even with the sample in vacuum. In addition to the hole where the focused laser had directly burnt, a faint inner ring and a clear-cut outer ring both concentric to the central burnt hole were formed.

For a cross-sectional view of the crater, we performed (in vacuum) LII in an aligned CNT array at a spot near the edge of the sample. The sample was then taken out of the vacuum chamber and laser pruning was performed in room ambient condition to burn away one half of the crater, as shown in Fig. 5(a). Cross-sectional view of the crater presented in Fig. 5(b) shows that the outer ring boundary, as seen from top-view, was due to deep surface cracks in the array. Figures 5(c) and 5(d) shows the magnified images of portions of the outer ring to the left and right sides of the central hole, respectively. We estimate the width of the cracks to be ~1–2 μm in width. Details of the faint inner ring are unfortunately not as clear.

Raman spectroscopy at different radial positions across the crater was carried out. Major peaks at 1343 and 1575 cm^{-1} correspond to the D (defective) and G (graphitic) bands, respectively. The ratio of the intensities at the two bands is often used as a measure of quality for CNT samples. As shown in the results displayed in Fig. 6, I_D/I_G within the crater is lower than that outside, indicating that the post-LII CNTs have less structural defects than as grown. We propose the high temperature generated during LII helped to burn away amorphous carbons on as-grown CNTs, leaving behind "cleaner" nanotubes. This is similar to the method of purifying CNTs by heat treatment.[24] We also find a consistent trend of lower I_D/I_G nearer to the center of the crater. This follows from the account where heat generated through LII burns away amorphous carbons on the CNTs. Since the heat near the center will be more intense, more amorphous carbons will be burnt and thus leads to lower I_D/I_G.

A dynamic study of the ring-pattern crater formation was carried out by performing LII of various durations at different spots on the same sample and studying their corresponding craters by scanning electron microscopy (SEM). Figure 7 shows that the ring pattern was not formed immediately upon laser irradiation, rather the first signs of formation of the outer ring shows after ~8 s. The outer ring boundary then slowly widens, working inwards such that the outer diameter of the crater remains constant with time.

The size of the crater varies with laser power—the higher the laser power, the larger the diameter of the crater. Such a trend is clearly displayed in Fig. 8. In our earlier paper, we showed that laser power correlates with the intensity of LII, but yet the temperature of LII showed little variation with laser power.[8] We concluded that higher laser powers do not significantly raise the incandescence temperature, but act to increase the number of incandescent CNTs. Our observations in Fig. 8 further support the point that a higher laser power heats a larger area of CNTs to the incandescent temperature. The CNTs that perform LII effectively radiate the energy pumped in from the laser beam such that the temperature is kept at ~2400 K and not increasing any further.

Based on the above investigations, we propose a mechanism for the formation of LII craters. CNTs under focused laser beam efficiently absorbed light energy and were instantly heated up. From the focused laser spot on the sample, heat spread radially out to surrounding CNTs by conduction in the entangled network of CNT forest, which raised the temperature to a point where incandescence took place. Just as heat is gained from neighboring CNTs nearer to the laser spot, heat is lost to neighboring CNTs further from the laser spot. The rate of net heat gain decreases with increasing radial distance from the laser spot. LII therefore occurs

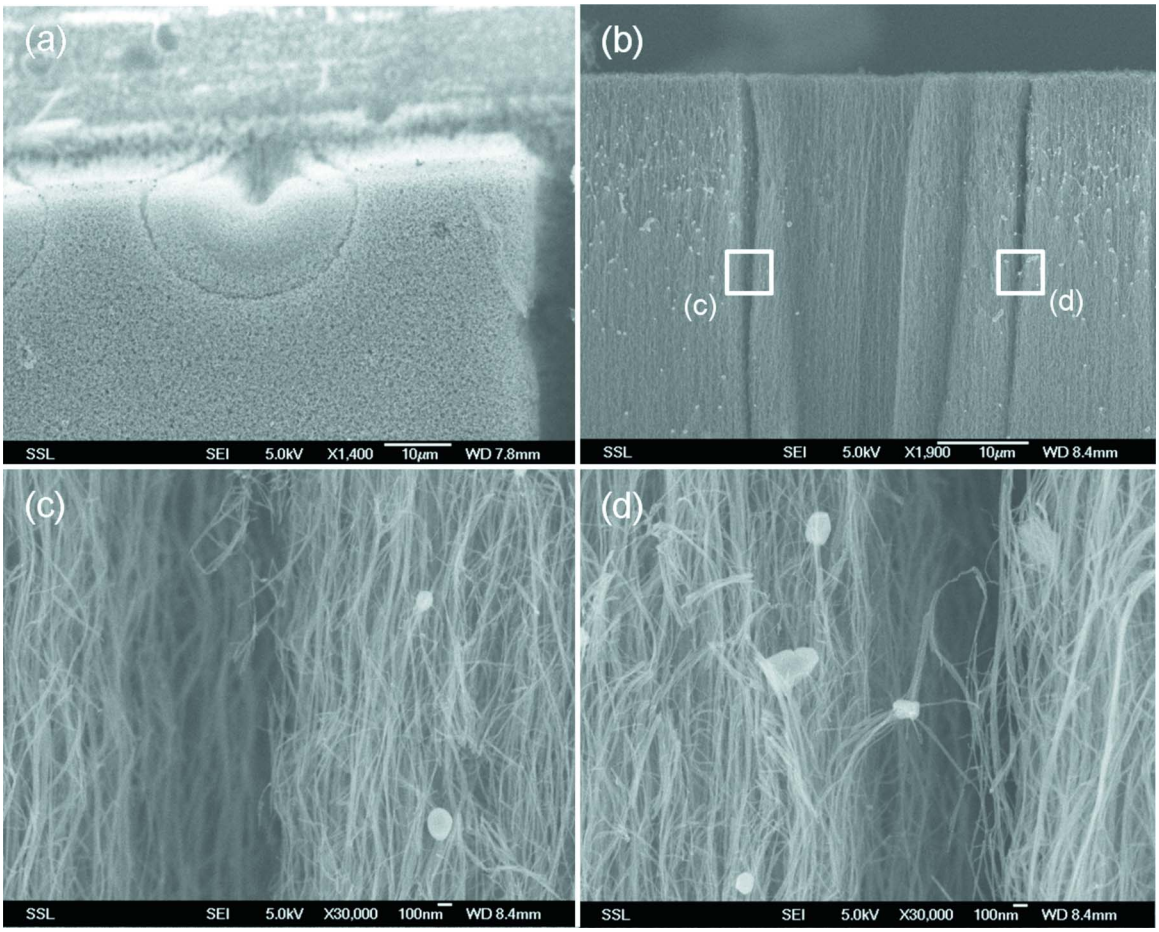

FIG. 5. (Color online) SEM images showing (a) top-view of an LII crater laser pruned to reveal its cross-section, (b) cross-sectional view of the crater, (c) and (d) magnified images of portions of the outer ring to the left and right sides of the central hole, respectively.

within an area of CNTs around the laser, beyond which the CNTs fail to reach the incandescent temperature. Due to the intense heat generated, CNTs performing LII may undergo other physical and chemical processes. Evidence from Raman spectroscopy suggests that the amorphous carbons were removed from the incandescent CNTs. This could have allowed these CNTs to be more tightly packed resulting in contraction of the CNT array. As more amorphous carbons were removed nearer to the laser spot, the array of incandescent CNTs contract inwards, inducing surface cracks, which eventually results in the formation of the outer ring boundary. Once the outer ring boundary is formed, heat loss to CNTs outside the crater is reduced. The incandescence then gradually burns the CNTs within the crater resulting in the slow widening of the outer boundary.

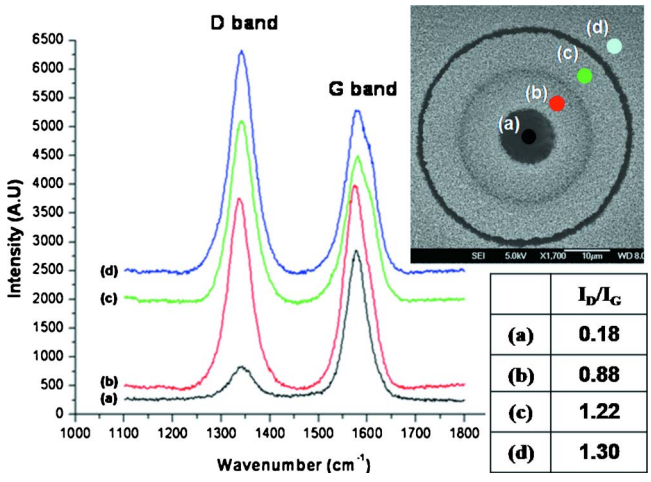

	I_D/I_G
(a)	0.18
(b)	0.88
(c)	1.22
(d)	1.30

FIG. 6. (Color online) Raman spectroscopy at various radial positions across the LII crater. Decreasing trend in the ratio of I_D vs I_G is observed as the laser beam scans toward the center of the crater.

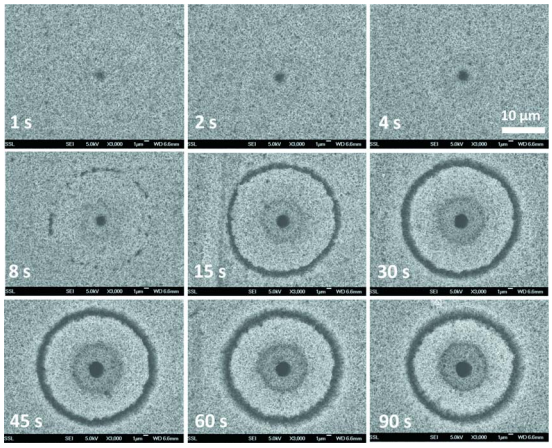

FIG. 7. (Color online) SEM images of craters formed by different durations of LII.

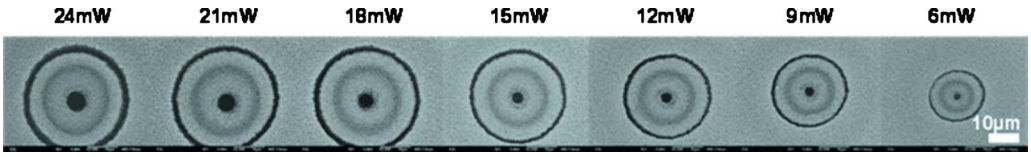

FIG. 8. (Color online) SEM images of craters formed by different laser powers.

C. Dependence of LII on air pressure

Detailed pressure variation study was carried out to study the dependence of LII on air pressure. LII experiments were conducted over a range of air pressures ranging from 1.4 to 120 mTorr with a fixed laser power of 24 mW. The vacuum chamber with a CNT sample in ambient air was first pumped down to the maximum vacuum level and a micrometer screw gauge valve was used to vary the air pressure for each experiment. Each run was carried out on a different location within the same sample of aligned multiwalled CNT array. The results, as shown in Fig. 9, are surprisingly rich. In the graph of Fig. 9, two general trends of LII profile were observed, one with a sudden peak and one that was sustained and showed little variations in intensity. These two trends are seen in inset (a) of Fig. 9. In general, the former occurred at high pressures while the latter occurred at low pressures. LII of CNTs at 2.6 mTorr pressure and lower were found to be highly sustained. We suggests that at low pressures, fewer gas molecules interacts with the CNTs and the laser-heated CNTs are allowed to maintain the high temperature incandescence process without being exhausted in possible chemical reactions with gaseous molecules in the environment. In addition, it was observed that at low pressures in particular, the average intensities of LII of CNTs increases with increasing pressure. A clearer picture of this trend can be seen in inset (b) of Fig. 9. Such a trend is attributed to the varying amount of gas molecules in the air. Interactions with gaseous molecules are believed to generate exothermic reactions, resulting in a greater extent of CNTs heated to the incandescent temperature. Conversely, the lower the pressure, the fewer the number of gas molecules in the air, the slower the rate of exothermic reactions with CNTs, thus the lower the intensities of LII by blackbody emission.

However, LII at high pressures (above 3.1 mTorr) gave rise to a very different yet interesting LII profile. These spectrums each have a sharp and sudden peak, which subsequently drops down to zero in a short while. This is in fact a thermal runaway where an exothermic reaction reaching a very high temperature perpetually increases the rate of subsequent reaction, causing this chain reaction to go out of control, eventually resulting in a small explosion (see video of thermal runaway during LII in Ref. 21). As a result, when all the CNTs are destroyed rapidly, incandescence signals drop to zero very quickly. This is believed to be due to the presence of more gas molecules at higher pressure. Since the exothermic reaction can occur at a very fast rate, more energy is generated for more intense burning to take place, sparking off the chain reaction that results in the small explosion depicted in the graph by a sudden peak in incandescence signal that subsequently drops to zero. At higher pressures beyond 120 mTorr, a thermal runaway can even be reached as soon as the laser irradiation starts and LII signals can drop drastically to 0 within 1 s.

It is also interesting to note that at high pressures, the sustainability of LII of CNTs, which in this context means the time taken by the CNTs to reach a thermal runaway de-

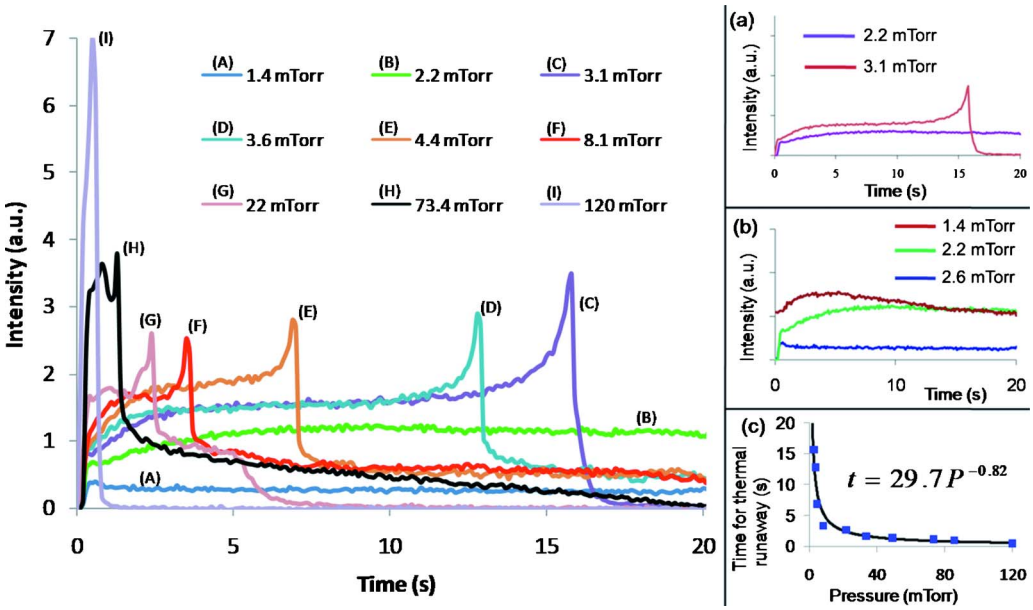

FIG. 9. (Color online) LII intensity at various operating pressures. Inset (a) shows two general trends—one with stable intensity and one with a sharp peak followed by an even sharper drop in intensity. Inset (b) shows that in higher vacuum, LII intensity increases with increasing laser power. Inset (c) sows that the time for thermal runaway to occur reduces for higher pressures.

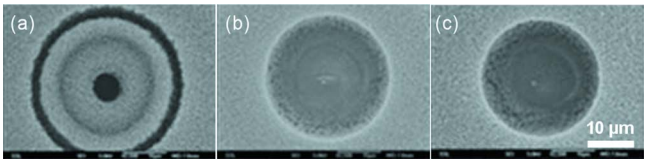

FIG. 10. (Color online) LII craters formed at (a) 1 mTorr, (b) 10 mTorr, and (c) 100 mTorr vacuum conditions. Massive destruction of CNTs is observed for (b) and (c).

creases with increasing pressure i.e., lower vacuum. This is again attributed to the varying amount of gas molecules at different pressures. The higher the pressure, the more gas molecules in the air, and the faster the rate of exothermic reactions with CNTs, thus the shorter time it takes for a thermal runaway to occur. This inverse relationship between the sustainability of LII of CNTs and the pressure conditions can be summarized as in inset (c) of Fig. 9.

The case of massive destruction of CNTs due to thermal runaway during LII is confirmed with post-LII SEM images of the craters formed at various pressures, as shown in Fig. 10. Clearly almost all the CNTs within the craters formed in 10 and 100 mTorr were destroyed.

D. Dependence of LII on gaseous environment

For a sustainable LII in CNTs array, it is important that thermal runaway do not occur. In view of this, we subject the CNTs in the vacuum cell to various gaseous environments, namely argon, carbon dioxide, nitrogen, and oxygen. The desired gas was flushed into the vacuum chamber for at least

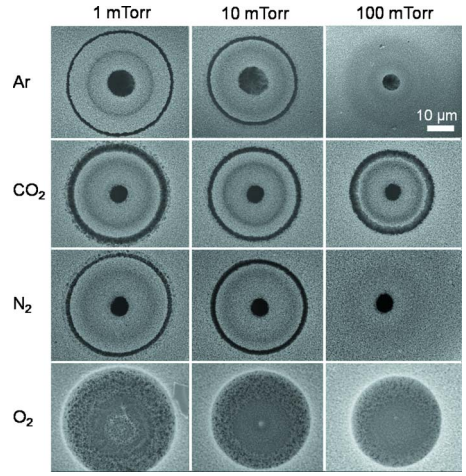

FIG. 12. (Color online) Craters formed during LII in various gaseous environments. Massive destruction of CNTs in oxygen shows that thermal runaway had occurred. In contrast, most of the CNTs in argon, carbon dioxide, and nitrogen gas survived to give sustained LII.

half an hour before each set of LII experiment in controlled environment was carried out. Figure 11 shows the evolution of LII at various pressures in different gaseous environments. Corresponding SEM images of post-LII are shown in Fig. 12. A glance at the results in Figs. 11 and 12 immediately point to oxygen as the gas responsible for the runaway reactions. CNTs in oxygen environment clearly exhibit thermal runaway during LII as apparent from the spike of intense LII and the rapid decay that follows. This is in contrast to the well sustained LII in argon, carbon dioxide, and nitrogen

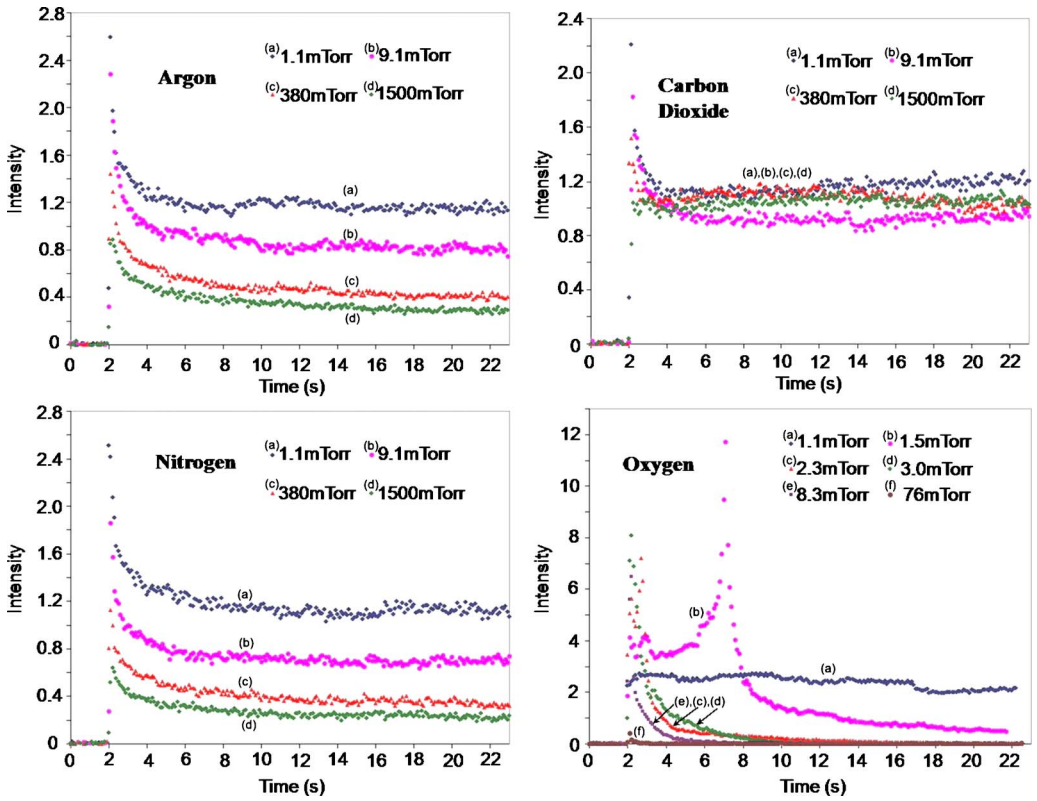

FIG. 11. (Color online) LII at various gaseous environments. Laser was irradiated on the samples after $t=2$ s. Thermal runaway do not occur in argon, carbon dioxide, and nitrogen gas environments even at low vacuum condition of 1.5 Torr. The display of thermal runaway in oxygen environment shows that oxygen is the gas responsible for thermal runaway during LII.

environments. Comparing Fig. 11 with the results in Fig. 9, we further note that thermal runaway in oxygen can occur at pressures as low as 1.5 mTorr while the phenomenon only occurred at pressures greater than 3.1 mTorr in normal air-composition vacuum. We also observe massive destruction of CNTs in the craters formed in oxygen environment in Fig. 12, clearly an aftermath of thermal runaway. Long sustainability of LII in argon and nitrogen gas environments is attributed to the inert nature of these gases. We also observe a trend of decreasing LII intensity with higher pressure. This is explained by the more efficient heat loss by conduction to the gaseous neighborhood at higher pressure conditions, resulting in a lesser extent of CNTs heated to incandescence. The decreasing size of post-LII craters with higher pressure as shown in Fig. 12 shows that less CNTs were heated to incandescence at higher pressure and thus supports the above explanation. The trends of LII in carbon dioxide gas differ from other gaseous environments. We believe that while carbon dioxide does not react with CNTs as readily as oxygen, it is not as inert as argon and nitrogen. The high temperature generated during LII may induce slow chemical reactions between carbon dioxide molecules.

IV. CONCLUSION

LII in aligned CNTs were investigated in details. We report the observation of LII craters with concentric ring patterns and examine the formation of these craters. A mechanism involving the burning of amorphous carbons during the high temperature process of LII and a contracting array of CNTs toward the center laser spot was proposed. Dependence of crater size on duration of LII, and laser power was explained. A detailed pressure dependence study revealed thermal runaway events for LII in pressures greater than 3 mTorr. While interesting in itself, thermal runaway posed a threat to a sustained LII due to the massive destruction of CNTs. Through experiments of LII in various controlled environments, we found oxygen as the gas responsible for the thermal runaway.

ACKNOWLEDGMENTS

The authors acknowledge the generous support of ASTAR under PMED TSRP Grant and Mr. Lim Kim Yong for useful discussions.

[1]G. Singh, P. Rice, K. E. Hurst, J. H. Lehman, and R. L. Mahajan, Appl. Phys. Lett. **91**, 033101 (2007).
[2]X. Bai, D. Li, D. Du, H. Zhang, L. Chen, and J. Liang, Carbon **42**, 2125 (2004).
[3]R. Z. Ma, B. Q. Wei, C. L. Xu, J. Liang, and D. H. Wu, Carbon **38**, 636 (2000).
[4]F. C. Cheong, K. Y. Lim, C. H. Sow, J. Lin, and C. K. Ong, Nanotechnology **14**, 433 (2003).
[5]S. Lu and B. Panchapakesan, Nanotechnology **18**, 305502 (2007).
[6]A. Fujiwara, Y. Maniwa, H. Suematsu, N. Ogawa, K. Miyano, H. Kataura, Y. Maniwa, S. Suzuki, and Y. Achiba, Jpn. J. Appl. Phys., Part 2 **40**, L1229 (2001).
[7]K. Y. Lim, C. H. Sow, J. Lin, F. C. Cheong, Z. X. Shen, J. T. L. Thong, K. C. Chin, and A. T. S. Wee, Adv. Mater. **15**, 300 (2003).
[8]Z. H. Lim, A. Lee, Y. Zhu, K. Y. Lim, and C. H. Sow, Appl. Phys. Lett. **94**, 073106 (2009).
[9]A. C. Eckbreth, J. Appl. Phys. **48**, 4473 (1977).
[10]L. A. Melton, Appl. Opt. **23**, 2201 (1984).
[11]R. L. Vander Wal and K. J. Weiland, Appl. Phys. B: Lasers Opt. **59**, 445 (1994).
[12]H. A. Michelsen, J. Chem. Phys. **118**, 7012 (2003).
[13]C. Schulz, Appl. Phys. B: Lasers Opt. **83**, 331 (2006).
[14]P. M. Ajayan, M. Terrones, A. Gaurdia, V. Huc, N. Grobert, B. Q. Wei, H. Lezec, G. Ramanath, and T. W. Ebbesen, Science **296**, 705 (2002).
[15]B. Bockrath, J. K. Johnson, D. S. Sholl, B. Howard, C. Matranga, W. Shi, D. Sorescu, P. M. Ajayan, G. Ramanath, M. Terrones, and T. W. Ebbesen, Science **297**, 192 (2002).
[16]Y. Zhang, T. Gong, W. Liu, X. Zhang, J. Chang, K. Wang, and D. Wu, Appl. Phys. Lett. **87**, 173114 (2005).
[17]S. Singamaneni, V. Shevchenko, and V. Bliznyuk, Carbon **44**, 2191 (2006).
[18]S. H. Tseng, N. H. Tai, W. K. Hsu, L. J. Chen, J. H. Wang, C. C. Chiu, C. Y. Lee, L. J. Chou, and K. C. Leou, Carbon **45**, 958 (2007).
[19]F. Tarazona-Vasquez and P. B. Balbuena, J. Phys. Chem. **112**, 4172 (2008).
[20]Y. H. Wang, J. Lin, C. H. A. Huan, and G. S. Chen, Appl. Phys. Lett. **79**, 680 (2001).
[21]http://www.physics.nus.edu.sg/~physowch/CNT_LII/CNT_LII.html
[22]P. Li, K. Jiang, M. Liu, Q. Li, S. Fan, and J. Sun, Appl. Phys. Lett. **82**, 1763 (2003).
[23]J. Wei, H. Zhu, D. Wu, and B. Wei, Appl. Phys. Lett. **84**, 4869 (2004).
[24]P. X. Hou, C. Liu, and J. M. Cheng, Carbon **46**, 2003 (2008).